Reversal of the Hofmeister Series: Specific Ion Effects on Peptides

Jana Paterová,[1] Kelvin B. Rembert,[2#] Jan Heyda,[3]Yadagiri Kurra,[2]Halil I. Okur,[2#]Wenshe R. Liu[2], Christian Hilty,[2] Paul S. Cremer,[2#*]and Pavel Jungwirth[1*]

[1]*Institute of Organic Chemistry and Biochemistry, Academy of Sciences of the Czech Republic, Flemingovo nám. 2, 16610, Prague 6, Czech Republic,* [2]*Department of Chemistry Texas A&M University, 3255 College Station, TX 77843, USA,* [3]*Soft Matter and Functional Materials, Helmholtz-Zentrum Berlin, Hahn-Meitner Platz 1, 14109 Berlin, Germany*.

[#]Current address: Chemistry Department, Penn State University, University Park, PA 16802

*Corresponding authors: psc@psu.edu (P.S.C.)and pavel.jungwirth@uochb.cas.cz

Keywords:peptides, ions, Hofmeister series, NMR, molecular dynamics.

Abstract

Ion specific effects on salting-in and salting-out of proteins, protein denaturation, as well as enzymatic activity are typically rationalized in terms of the Hofmeister series. Here, we demonstrate by means of NMR spectroscopy and molecular dynamics simulations that the traditional explanation of the Hofmeister ordering of ions in terms of their bulk hydration properties is inadequate. Using triglycine as a model system, we show that the Hofmeister series for anions changes from a direct to a reversed series upon uncapping the *N*-terminus. Weakly hydrated anions, such as iodide and thiocyanate, interact with the peptide bond, while strongly hydrated anions like sulfate are repelled from it. In contrast, reversed order in interactions of anions is observed at the positively charged, uncapped *N*-terminus, and by analogy, this should also be the case at side chains of positively charged amino acids. These results demonstrate that the specific chemical and physical properties of peptides and proteins play a fundamental role in ion specific effects. The present study thus provides a molecular rationalization of Hofmeister ordering for the anions. It also provides a route for tuning these interactions by titration or mutation of basic amino acid residues on the protein surface.

Introduction

Traditional rationalization of specific ion effects on proteins has been based on dividing ions into kosmotropes and chaotropes[1, 2]. Within this picture, the strongly hydrated kosmotropes are assumed to be able to organize a significant number of water molecules around themselves[3] and effectively "steal" water from protein molecules. Therefore, they

salt-out proteins from aqueous solutions. By contrast, weakly hydrated chaotropes are not able to effectively organize water molecules around themselves. Thus, they are supposed to "lend" water molecules to proteins, which facilitates their hydration[4]. There are, however, at least two serious problems with these explanations[5-7]. First, spectroscopic experiments and molecular simulations show that biologically relevant ions can strongly influence only their immediate solvation shell and do not show any long-range kosmotropic effects in water[8, 9]. Second, the usual ordering of ions according to their ability to salt out proteins, i.e., the Hofmeister series[10, 11], becomes reversed in certain cases[12]. The best known example is lysozyme, which behaves according to the regular Hofmeister series only at high pH or high ionic strength. Under neutral and acidic conditions, its salting out behavior actually follows a reversed ionic series[11-14].

The first observation suggests that we may have to abandon the notion of kosmotropes and chaotropes, since these words are connected with the unsubstantiated concept of long-range water ordering by ions. The second issue points to the importance of the physical and chemical properties of the protein itself, which should not be neglected. In other words, we cannot hope to explain ion specific effects on proteins and the corresponding Hofmeister series by describing only the behavior of the aqueous ions, since proteins or peptides play an integral role in the process. In fact, previous investigations aimed at quantifying the interactions of Hofmeister anions with model compounds, such as acetamide and individual amino acids[15-21]. Remarkably, already in the 1960s and 70s, Robinson et al. studied the effects of salts on small oligopeptides, including diglycine, triglycine, and tetraglycine[15, 16, 21]. Unfortunately, the conclusions of their work

wereaffected by the erroneous assumption that the *C*-terminus of oligoglycines could be easily esterified (*vide infra*).

In the present study, we carefully investigate the interactions of Hofmeister anions with triglycine (GGG) by NMR spectroscopy and molecular dynamics (MD) simulations. We show that when the end groups of the peptide are capped, anion interactions with the backbone are stronger for large soft ions compared with small hard ions possessing a higher charge density. This is consistent with a direct Hofmeister series according to the principle that ions repelled from the surface of the peptide or protein cause these molecules to salt-out of solution, while ions exhibiting affinity for the peptide salt it in[17, 22].In contrast, when the peptide is uncapped, interactions with the positively charged *N*-terminus lead to a reversed series for anions. Thus, Hofmeister ordering for anions turns out to be a complex effect involving multiple interactions with the peptide. These effects can be finely tuned or even reversed by making simple changes to the peptide's chemistry.

Methods and Materials

Computational method. The triglycine peptide (capped or uncapped), described with the polarizable version of the parm99SB force field[23], was solvated in 1 M NaX (X = Cl, Br, or I)[24, 25],1 M NaSCN[26], or in 0.333 M Na_2SO_4 [27] (i.e., employing the same ionic strength for all solutions). The simulated unit cell of approximately43 × 43 × 43 $Å^3$consisted of a single tripeptide, 2503POL3 water molecules[28], 45 cations, and 45 anions (or 30 cations and 15 anions for sulfate). 3D periodic boundary conditions were applied with long-range electrostatic interactions beyond the non-bonded cutoff of 8 Å accounted for using the

particle mesh Ewald (PME) method[29].All bonds containing hydrogens were constrained using the SHAKE algorithm[30].The system was held at ambient conditions (300 K and 1 atm) by coupling to the Berendsen barostat and thermostat[31]. The total simulation time for each system was 100 ns (after 1 ns of equilibration), with a time step of 1 fs. Coordinates were saved every 1 ps, yielding 10^5 frames for further analysis, from which we selected ~60 % frames corresponding to extended peptide geometries (for sake of easier analysis in terms of density maps). Polarizable MD calculations were performed using the AMBER11 program[32].

Analysis of MD data. Simulation data were analyzed in two ways. First, the analysis was done in terms of spatial distribution functions $\rho(\mathbf{r})$ of ions, performed on a subset of extended GGG conformations. The three-dimensional nature of this function allows us to visualize it only at certain isolevel, i.e.,encompassing regions where the local density is above a given threshold. Note that a spatial distribution function can be reduced to a standard radial distribution function via integration over the two angular coordinates.

Second, we calculated the proximal distribution functions for ions and water, $g_{prox}(r)$. The proximal character is here preferred to the standard radial distribution function, since the peptide is a non-spherical object and such an analysis allows us to distinguish affinities to different regions of GGG. In particular, here we dissect the GGG peptide into three regions corresponding to the individual residues, each containing one of the α-protons monitored by NMR (*vide infra*). For the proximal distribution function we monitor for each ion or water molecule the distances from all regions, with contribution to the distribution function made only to the closest region. The proximal distribution function for an ion to a

given group is calculated as

$g_{prox}^{ion-group}(r) = \frac{N_{prox}^{ion-group}(r+dr) - N_{prox}^{ion-group}(r)}{\rho_0^{ion}(V_{prox}^{group}(r+dr) - V_{prox}^{group}(r))}$, where the numerator is the number of ions in a layer within the given group at a distance *(r, r+dr)*, calculated from the difference between proximal numbers $N_{prox}^{ion-group}$ at r+dr and r,and the denominator is the bulk density times the layer volume of the group within the distance *(r, r+dr)*.Thus it is a ratio of proximal and bulk densities of an ion. Similarly to ions, a proximal distribution function can also be defined for water molecules.

The preferential binding coefficients Γ can be then calculated as

$$\Gamma^{group}(r) = N_{prox}^{ion-group}(r) - N_{prox}^{water-group}(r) \cdot \frac{N_{total}^{water}(r) - N_{prox}^{water-group}(r)}{N_{total}^{ions}(r) - N_{prox}^{ion-group}(r)}.$$

The preferential binding coefficient thus distinguishes between preferential binding of ions, Γ> 0, vs. preferential hydration,Γ< 0. A thermodynamic property is not the functionΓ(r) itself, but its limiting value at large distances. In our calculations we approximate this limit by the value at the plateau region at a distance of 12Å.The sums of the preferential binding coefficients of cations and anions must equal to each other to satisfy the electroneutrality condition, which can also be used as a self-consistency check of the chosen cut off distance and convergence of the simulation.

Materials. Glycylglycylglycine was purchased from Alfa Aeasar and used as received (99%, Ward Hill, MA). The synthesis of *N*-acetyltriglycinamide was performed by starting from an *N*-acetyldiglycine precursor[33, 34]. Specifically, diglycine was modified by acetylation of its *N*-terminus, followed by conjugation with glycinamide. The NaSCN, NaI,

NaBr, and Na_2SO_4employed in the NMR experiments was purchased from Sigma Aldrich (St. Louis,MO), while NaCl came from VWR (Radnor, PA). All salts were atleast 98% pure, and employing higher purity salts did not change the NMR spectra. 18.2MΩ·cm purified water from a NANO pure Ultrapure Water system (Dubuque, IA) was used to prepare salt and peptide solutions. Stock solutions of salts and peptides were prepared separately at double the desired concentration and mixed together in a 1:1 (volume to volume) ratio to obtain the desired sample concentration. The total peptide concentration in all experiments was 50 mM. More details of the synthesis and characterization of the capped-GGG molecule are provided in the Supporting Information section.

NMR Titrations. All spectra were acquired on a 400 MHz spectrometer equipped with a 5 mm TXI probe (Bruker, Billerica, MA) at a temperature of 298 K. For chemical shift assignments of the peptides, spectra employed were [1H,1H]-NOSEY (100 ms mixing time for GGG and 250 ms mixing time for N-Ac-GGG-NH2) and [1H,1H]-TOCSY (100 ms mixing time)[35], as well as [13C,1H]-HSQC and [13C,1H]-HMBC (J-filter range between 5 and 14 Hz)[36].TopSpin software (Bruker) was used for data processing. For titrations of peptides with salts, 1H NMR spectra were acquired using presaturation or watergate for water suppression[37]. Sample spectra were externally referenced to sodium 2,2-dimethyl-2-silapentane-5-sulfonate (DSS) (Cambridge Isotope Laboratories) in pure D_2O (99.9% D, Cambridge Isotope Laboratories) in NMR tubes adapted with coaxial inserts (Wilmad-LabGlass). The DSS was always in the inner of the concentric tubes, while the peptide sample was in the outer tube. The DSS reference was never exposed to the peptide or varying salt concentrations.

Results

Computational

We performed polarizable MD simulations of triglycine in aqueous solutions of five sodium salts - Na_2SO_4, NaCl, NaBr, NaI, and NaSCN. The 1 M salt concentration and 100 ns simulation length ensured converged distributions of ions around the peptide. Figure 1 depicts the ion density maps around the capped and uncapped triglycine, which directly show the averaged distributions for each system. For the chosen isovalue, the contours presented in the figure correspond to regions with ion concentration enhanced by a factor of three with respect to the bulk aqueous solution. Figures 2 and 3 show the resulting proximal distribution functions and preferential binding of SO_4^{2-}, Cl^-, Br^-, I^-, and SCN^- to the regions around each of the three backbone CH_2groups(probed by NMR– *vide infra*) for both capped (Figure 2) and uncapped (Figure 3) triglycine. Note that the first region encompasses the *N*-terminus, while the third one contains the *C*-terminus. A proximal distribution function represents the probability of finding particular ions at a given distance from the investigated functional group on triglycine, while preferential binding is an integral quantity, which characterizes the affinity of the ion with respect to water for a given functional group within a specified distance. If the preferential binding converges over large distances to a positive value, there is a net attraction of the ion to the functional group of the peptide. If, however, it converges to a negative value, then there is a net repulsion and the functional group is preferentially hydrated instead.

Figures 1 and 2 demonstrate that the total affinities for the anions with capped

triglycine follow a direct Hofmeister series: SO_4^{2-}<Cl^-< Br^-< I^-< SCN^-. This is consistent with standard salting-out behavior. Sulfate exhibits no net preferential binding for the amide or CH_2 groups on the peptide backbone, neither is it attracted to the capped *N*-terminus. In total, sulfate is thus repelled from the capped tripeptide. Chloride and bromide show virtually no preferential binding to the peptide and, therefore, act essentially as Hofmeister-neutral ions. In contrast, iodide exhibits some affinity for the backbone CH_2 groups. This affinity becomes even stronger for thiocyanate, particularly close to the *N*-terminus. The last two ions, therefore, behave as salting-in agents with SCN^- having a stronger effect than I^- at comparable concentrations.

The situation with ion affinities is more complex for the uncapped peptide (Figures 1 and 3). Unlike the case of the capped peptide, where the terminal groups play a negligible role in ion affinities, the positively charged *N*-terminus of the uncapped peptide dominates the anion interaction behavior. Sulfate exhibits a strong affinity for the charged *N*-terminus, followed by weaker interactions for chloride and the heavier halides. Interestingly, the non-spherical, internally structured thiocyanate anion does not quite follow the ionicseries in this respect, having a stronger affinity for the charged *N*-terminus than the halide anions.

NMR Spectroscopy

The chemical shifts from NMR experiments of the three backbone methylene units of capped triglycine were monitored as a function of salt concentration for the same five sodium salts as in the MD simulations (Figure 4). The top plot in each vertical pair of diagrams represents the total chemical shift observed as a function of salt concentration.

These data can be fit to the following equation:

$$\Delta\delta = -c[M] + \frac{\Delta\delta_{\max}[M]}{K_D + [M]} \ .$$

This type of fitting is typical for the salt concentration dependence of the physical behavior of surfactants, colloids, and biomolecules in solution and has been described elsewhere in detail. [5,13] The linear portion is usually attributed to a bulk effect, while the nonlinear portion should correspond to saturation binding behavior.

The lower plot shows the data after the linear portion of the data has been subtracted[38]. As can be seen, the data fit very well to a Langmuir isotherm for I^- and SCN^- at the CH_2 group next to the capped *N*-terminus (α-proton 1) and for SCN^- at the middle glycine (α-proton 2); the three K_D values are provided in Table 1. These interactions for the anions with the peptide are in agreement with those observed above by MD simulations. No appreciable binding was observed with any of the anions at the α-proton 3, which was close to the *C*-terminus. Moreover, only linear behavior was observed for Cl^- and Br^- at all the probed sites. There were, however, nonlinear changes associated with the chemical shifts of SO_4^{2-} at all three positions (Figure 4). While these latter curves exhibit non-linear behavior, they show opposite curvature from those of the weakly hydrated anions. As such, the curvature may not originate from direct ion-peptide interactions, or even from changes in the peptide secondary structure. Indeed, infrared data of the amide bands for capped GGG in D_2O with 1 M Na_2SO_4 show no peak shifts or intensity changes within experimental error compared with the peptide in pure D_2O (Supporting Information).Therefore, neither FTIR nor MD data support the idea that SO_4^{2-} binds or causes substantial changes to the

secondary structure. Instead, the NMR curves with SO_4^{2-} may reflect the anion's repulsion from the peptide's immediate solvation shell, as observed in MD simulations. Such exclusion could lead to water restructuring in the region between the peptide and SO_4^{2-} and, consequently, to the non-linear NMR shifts that we observed. It also may be responsible for the opposite curvature seen in the NMR data compared with iodide and thiocyante. Thus, the results from Figure 4 should be consistent with a direct Hofmeister series. Namely, only the most weakly hydrated ions, thiocyanate and iodide, bind to the uncharged glycine residues while the other anions do not.

In a second set of experiments, analogous chemical shifts as above were monitored with uncapped triglycine molecules (Figure 5). The chemical shifts varied with salt concentration for all three methylene units. However, there were remarkable differences between the individual α-protons. For the methylene group adjacent to the positively charged *N*-terminus, all the chemical shifts varied in a non-linear fashion (Figure 5, α-proton 1, top). When the linear part was subtracted out, Langmuir binding isotherms were revealed in the presence of all five sodium salts (Figure 5, α-proton 1, bottom). In this case, SO_4^{2-} displayed the tightest K_D value, while I^- displayed the weakest (Table 1). More specifically, the ordering was SO_4^{2-}>Cl^-> Br^-> SCN^-> I^-. This is a completely reversed Hofmeister series except for thiocyanate, which again exhibits stronger binding than iodide. By contrast, the chemical shift of the protons associated with the middle methylene unit (α-proton 2) and the methylene unit adjacent to the negatively charged *C*-terminus (α-proton 3) showed much less nonlinear variation with added salt for all the monovalent anions. At these two sites, only the α-proton 2 data could be fit to a Langmuir isotherm when varying

the SCN^- concentration and the binding constant in this case was weaker than that found at α-proton 1 (Table 1). SO_4^{2-} showed the same type of changes in the chemical shift at α-protons 2 and 3 as that found with the capped version of the peptide. Again, this may represent solvent shell reorganization upon depletion of SO_4^{2-} from the immediate vicinity of the peptide.

Discussion

The principal result of the present study is the change from direct to reversed Hofmeister series of anions, observed both by NMR and MD simulations, induced by uncapping the terminal group of the triglycine peptide. In the case of capped triglycine, the interaction sites for anions are at the backbone, which attracts the weakly hydrated thiocyanate and iodide anions, but not the more strongly hydrated smaller halides or sulfate. For uncapped triglycine, the situation is very different (see schematic Figure 6 for aqualitative comparison between these two cases). As can be clearly seen from both NMR measurements and MD simulations, the binding of anions is dominated by the influence of the positively charged *N*-terminus of the uncapped tripeptide. With the possible exception of SCN^- interacting with the middle methylene unit, no evidence can be found for appreciable anion binding at other portions of the peptide and we find a clear repulsion in the vicinity of the negatively charged *C*-terminus. Most importantly, ion-pairing interactions between the positively charged amine group at the *N*-terminus and the anions follow a *reversed* Hofmeister series: $SO_4^{2-} > Cl^- > Br^- > I^-$. The only partial outlier is SCN^-, which should be Hofmeister-ordered to the right of iodide, but actually exhibits stronger binding. The NMR results place it between Br^- and I^-, while the MD simulations predict

even stronger binding of SCN^- to the positively charged *N*-terminus. This small difference between the simulations and the NMR measurements could be due to the fact that the latter does not directly probe the binding site but rather at the adjacent methylene group (α-proton 1).It is also possible, that MD slightly overestimates SCN^- binding due to potential inaccuracies in the force field.

We note that the above ionic ordering does not obey the empirical "law of matching water affinities" in this particular case[1].This would have predicted that more weakly hydrated ions like I^-should interact more strongly with the putatively weakly hydrated amine group of the positively charged *N*-terminus than the more strongly hydrated monovalent anions, such as Cl^-. We have recently shown that depending on the molecular context, the amine group can vary in its hydration strength[39]. In this respect, the *N*-terminus of triglycine falls on the side of strongly hydrated cations.This is a somewhat different situation from that in a single amino acid (glycine), where the close proximity of the anionic *C*-terminus results in weaker and roughly comparable interactions of the *N*-terminus with strongly (F^-) and weakly (I^-) hydrated anions[39]. The present results also shed new light on a recent study of uncapped triglycine which concluded that strongly hydrated anions rather than weakly hydrated anions interact with the polypeptide backbone[40]. That conclusion was, however, based on a set of only two anions - sulfite and bromide, where several problems arise. First, sulfite quickly equilibrates with bisulfite in aqueous solution, leading to a mixture of both the weakly (bisulfite) and strongly (sulfite) hydrated anions. The protonation of sulfite also causes the pH of the solution to become basic. Second, bromide is near the middle of the Hofmeister series and does not represent the behavior of

weakly hydrated anions such as I^-, SCN^-, or ClO_4^-. Additionally, simulations did not completely match the corresponding X-ray absorption data for triglycine-salt interactions. Finally, MD simulations of the system indicated that the peptide underwent comformational changes.[40] However, herein we found that no appreciable comformational changes occur in these salt solutions (see Table S3 in SI) when simulations are done with a sufficent number of surrounding water molecules.

In terms of chemical synthesis, capping the *N*-terminus of triglycine was found to be straightforward, but capping of the *C*-terminus proved to be more difficult. In fact, the *C*-terminus could not be effectively capped by previously described esterification procedures[16, 21]. Further attempts to amidate the *C*-terminus also proved to be unsuccessful. The appropriately terminated molecule could be formed, however, by reacting acetylated diglycine with glycinamide. Both ESI-TOF mass spectrometry and proton NMR confirmed the correct structure under these conditions (see Supporting Information for additional details). The problem of efficiently capping the *C*-terminus with standard esterification chemistry has only secondary relevance for the present investigations of anionic interactions. It is, however, significant for cationic binding since the partially capped triglycine possesses a negatively charged *C*-terminus. This was, in fact, the species that interacted with Na^+ in early solubility experiments from Robinson et al.[16, 21]. Also, their attempts to infer ion interactions with the individual glycine units by varying the length of a partially capped oligoglycine may have suffered from variations in the secondary structure as the molecule was lengthened from diglycine to pentaglycine. The current findings call

for a critical reexamination of the ion partitioning coefficients from Robinson et al., used in later thermodynamic models of Hofmeister effects[17].

The fact that the rank ordering of the Hofmeister series for anions can be reversed by uncapping the peptide has crucial consequences for the interpretation of ion specific effects. For both the capped and uncapped peptide, the aqueous solvent and the ions are the same. This means that Hofmeister ordering cannot be explained by considering only the ions and water molecules, but the interactions of ions with the peptide have to be brought into the picture and are actually decisive. Uncapping the *N*-terminus may be less relevant for larger proteins than for a tripeptide; however, the same cationic amine group is also present in the side chains of lysine residues. Similarly, the other two basic amino acids – arginine and (protonated) histidine have cationic groups which interact with anions in the same order as lysine[18]. Thus, an analogous Hofmeister reversal as induced here by uncapping a tripeptide can be observed in proteins by titration (or mutations) leading to an increased number of basic surface residues[11-13]. Moreover, the binding of weakly hydrated anions is enhanced in larger peptides and proteins compared to the present case due to the partial dehydration of the backbone groups and the presence of the low dielectric region of the protein core[38, 41]. Indeed, for elastin-like polypeptides consisting of 600 residues, we have recently demonstrated that both SCN^- and I^- interacted with the backbone with apparent K_D values on the order of 50 to 300 mM[38]. Importantly, such interactions were also found at GGG motifs in the middle of the long polypeptide chain. As such, it appears that, in addition to local chemical identity, the size and structure of the surrounding polypeptide also play an important role in the strength of anion interactions. In particular,

weakly hydrated anions should be more excluded from small peptides like triglycine compared with the macromolecule/water interface[42], since the former are completely surrounded by water.

Conclusions

A combined NMR and MD study of ion interactions with capped and uncapped triglycine demonstrates that the Hofmeister ordering of anions reverses upon uncapping the peptide. Namely, the capped peptide follows a direct Hofmeister series, with weakly hydrated ions (e.g., iodide and thiocyanate) interacting with the peptide bond and strongly hydrated ions (e.g., sulfate) being repelled from it. For the uncapped peptide, the rank order of anion binding reverses (with the only outlier being thiocyanate) due to interactions at the positively charged, uncapped *N*-terminus. The same ordering of the anions is also inferred for interactions with the positively charged side chains of lysine, arginine, and (protonated) histidine. The present case study of Hofmeister reversal demonstrates that ion specific effects on peptides and proteins cannot be rationalized solely in terms of hydration properties of individual ions. Interactions of ions with functional groups on the peptide play a key role in the physical properties of the system and a quantitative description of these interactions is crucial for understanding ion specific behavior. This work thus provides a molecular level basis for the observed Hofmeister reversals in proteins by pH titration or mutation of basic amino acid residues. It also provides a conceptual framework for devising strategies for manipulating protein properties, such as solubility or enzymatic activity, by interactions with specific salt ions.

Acknowledgments

P.J. thanks the Czech Science Foundation (GrantP208/12/G016) for support and acknowledges the Academy of Sciences for the Praemium Academie award. J.P. acknowledges support from the International Max-Planck Research School. P.S.C. thanks the Welch Foundation (A-1421) and the National Science Foundation (CHE-0094332). C.H. thanks the Welch Foundation (No. A-1658).Y. K. was partly supported by Welch Grant A-1715 to W.R.L.

Supporting Information provides details on sample preparation and NMR and FTIR measurements. This material is available free of charge via the Internet at http://pubs.acs.org.

References

1. Collins, K. D., Neilson, G. W., and Enderby, J. E. Ions in water: Characterizing the forces that control chemical processes and biological structure, *Biophys. Chem.* **2007**,*128*, 95-104.
2. Lo Nostro, P., and Ninham, B. W. Hofmeister Phenomena: An Update on Ion Specificity in Biology, *Chem. Rev.*, **2012**,*112*, 2286-2322.
3. Gumey, R. W. *Ionic Processes in Solution*, McGraw-Hill, New York, 1953.
4. Long, F. A., and McDevit, W. F. Activity coefficients of nonelectrolyte solutes in aqueous salt solutions, *Chem. Rev.* **1952**, *51*, 119-169.
5. Zhang, Y. J., and Cremer, P. S. Interactions between macromolecules and ions: the Hofmeister series, *Curr. Opin. Chem. Biol.* **2006**, *10*, 658-663.
6. Jungwirth, P., and Winter, B. Ions at aqueous interfaces: From water surface to hydrated proteins, *Annu. Rev. Phys. Chem.* **2008**, *59*, 343-366.
7. Kunz, W. Specific ion effects in colloidal and biological systems, *Curr. Opin. Colloid & Interface Sci.* **2010,***15*, 34-39.
8. Omta, A. W., Kropman, M. F., Woutersen, S., and Bakker, H. J. Negligible effect of ions on the hydrogen-bond structure in liquid water, *Science* **2003**, *301*, 347-349.
9. Funkner, S., Niehues, G., Schmidt, D. A., Heyden, M., Schwaab, G., Callahan, K. M., Tobias, D. J., and Havenith, M. Watching the Low-Frequency Motions in Aqueous Salt Solutions: The Terahertz Vibrational Signatures of Hydrated Ions, *J. Am. Chem. Soc.* **2012**, *134*, 1030-1035.
10. Hofmeister, F. Zur Lehre von der Wirkung der Salze, *Arch. Exp. Pathol. Pharmakol.* **1888**, *24*, 247-260.

11. Kunz, W., Henle, J., and Ninham, B. W. 'Zur Lehre von der Wirkung der Salze' (about the science of the effect of salts): Franz Hofmeister's historical papers, *Curr. Opin. Colloid & Interface Science* **2004**, *9*, 19-37.

12. Schwierz, N., Horinek, D., and Netz, R. R. Reversed Anionic Hofmeister Series: The interplay of Surface Charge and Surface Polarity, *Langmuir* **2010**, *26*, 7370-7379.

13. Zhang, Y. J., and Cremer, P. S. The inverse and direct Hofmeister series for lysozyme, *Proc. Natl. Acad. Sci. USA* **2009**, *106*, 15249-15253.

14. Lund, M., and Jungwirth, P. Patchy proteins, anions and the Hofmeister series, *J. Phys.-Condensed Matt.* **2008**, *20*, 11582.

15. Nandi, P. K., and Robinson, D. R. Effects of salts on free-energies of nonpolar groups in model peptides, *J. Am. Chem. Soc.* **1972**, *94*, 1308-1315.

16. Nandi, P. K., and Robinson, D. R. Effects of Salts on Free-Energy of Peptide Group, *J. Am. Chem. Soc.* **1972**, *94*, 1299-1308.

17. Pegram, L. M., and Record, M. T. Thermodynamic origin of Hofmeister ion effects, *J. Phys. Chem. B* **2008**, *112*, 9428-9436.

18. Heyda, J., Hrobarik, T., and Jungwirth, P. Ion-Specific Interactions between Halides and Basic Amino Acids in Water, *J. Phys. Chem. A* **2009**, *113*, 1969-1975.

19. Heyda, J., Vincent, J. C., Tobias, D. J., Dzubiella, J., and Jungwirth, P. Ion Specificity at the Peptide Bond: Molecular Dynamics Simulations of N-Methylacetamide in Aqueous Salt Solutions, *J. Phys. Chem. B* **2010**, *114*, 1213-1220.

20. Algaer, E. A., and van der Vegt, N. F. A. Hofmeister Ion Interactions with Model

Amide Compounds, *J. Phys. Chem. B* **2011**, *115*, 13781-13787.

21. Robinson, D. R., and Jencks, W. P. Effect of concentrated salt solutions on activity coefficient of acetyltetraglycine ethyl ester, *J. Am. Chem. Soc.* **1965**, *87*, 2470-2479.

22. Pegram, L. M., Wendorff, T., Erdmann, R., Shkel, I., Bellissimo, D., Felitsky, D. J., and Record, M. T. Why Hofmeister effects of many salts favor protein folding but not DNA helix formation, *Proc. Natl. Acad. Sci. USA* **2010**, *107*, 7716-7721.

23. Wang, J. M., Wolf, R. M., Caldwell, J. W., Kollman, P. A., and Case, D. A. Development and testing of a general amber force field, *J. Comput. Chem.* **2004**, *25*, 1157-1174.

24. Perera, L., and Berkowitz, M. L. Many-Body Effects in Molecular-Dynamics Simulations of Na+(H2o)N and Cl-(H2o)N Clusters, *J. Chem. Phys.* 1991, *95*, 1954-1963.

25. Perera, L., and Berkowitz, M. L. Structures of Cl-(H2o)(N) and F-(H2o)(N) (N=2,3,...,15) Clusters - Molecular-Dynamics Computer-Simulations, *J. Chem. Phys.* **1994**, *100*, 3085-3093.

26. Petersen, P. B., Saykally, R. J., Mucha, M., and Jungwirth, P. Enhanced concentration of polarizable anions at the liquid water surface: SHG spectroscopy and MD simulations of sodium thiocyanide, *J. Phys. Chem. B***2005**, *109*, 10915-10921.

27. Wernersson, E., and Jungwirth, P. Effect of Water Polarizability on the Properties of Solutions of Polyvalent Ions: Simulations of Aqueous Sodium Sulfate with Different Force Fields, *J. Chem. Theor. Comput.* **2010**, *6*, 3233-3240.

28. Caldwell, J. W., and Kollman, P. A. Structure and Properties of Neat Liquids Using

Nonadditive Molecular-Dynamics - Water, Methanol, and N-Methylacetamide, *J. Phys. Chem.* **1995**, *99*, 6208-6219.

29. Essmann, U., Perera, L., Berkowitz, M. L., Darden, T., Lee, H., and Pedersen, L. G. A Smooth Particle Mesh Ewald Method, *J. Chem. Phys.* **1995**, *103*, 8577-8593.

30. Ryckaert, J. P., Ciccotti, G., and Berendsen, H. J. C. Numerical-Integration of Cartesian Equations of Motion of a System with Constraints - Molecular-Dynamics of N-Alkanes, *J. Comput. Phys.* **1977**, *23*, 327-341.

31. Berendsen, H. J. C., Postma, J. P. M., Vangunsteren, W. F., Dinola, A., and Haak, J. R. Molecular-Dynamics with Coupling to an External Bath, *J. Chem. Phys.* **1984**, *81*, 3684-3690.

32. Case, D. A.; Darden, T. A.; Cheatham, III, T. E; Simmerling, C. L.; Wang, J.; Duke, R. E.; Luo, R.; Walker, R. C.; Zhang, W.; Merz, K. M. et al. AMBER 11, 2010, University of California, San Francisco.

33. Kim, K. H., Martin, Y., Otis, E., and Mao, J. Inhibition of I-125-labeled ristocetin binding to micrococcus-luteus cells by the peptides related to bacterial-cell wall mucopeptide precursors - quantitative structure activity relationships, *J. Med. Chem.* **1989**, *32*, 84-93.

34. Wu, X. X., Wu, X. F., Hou, Y. M., Ng, S. W., and Tiekink, E. R. T. Methyl 2-(4-chloro-3,5-dinitrobenzamido)acetate, *Acta Crystallographica E* **2011**, *67*, O3486-U3659.

35. Wutrich, K. *NMR of Proteins and Nucleic Acids*, Wiley-Interscience, New York, 1986.

36. Hadden, C. E., Martin, G. E., and Krishnamurthy, V. V. Improved performance

accordion heteronuclear multiple-bond correlation spectroscopy - IMPEACH-MBC, *J. Magnetic Resonance* **1999**, *140*, 274-280.

37. Liu, M. L., Mao, X. A., Ye, C. H., Huang, H., Nicholson, J. K., and Lindon, J. C. Improved WATERGATE pulse sequences for solvent suppression in NMR spectroscopy, *J. Magnetic Resonance* **1998**, *132*, 125-129.

38. Rembert, K. B., Paterova, J., Heyda, J., Hilty, C., Jungwirth, P., and Cremer, P. S. Molecular Mechanisms of Ion-Specific Effects on Proteins, *J. Am. Chem. Soc.* **2012**, *134*, 10039-10046.

39. Mason, P. E., Heyda, J., Fischer, H. E., and Jungwirth, P. Specific Interactions of Ammonium Functionalities in Amino Acids with Aqueous Fluoride and Iodide, *J. Phys. Chem. B* **2010**, *114*, 13853-13860.

40. Schwartz, C. P., Uejio, J. S., Duffin, A. M., England, A. H., Kelly, D. N., Prendergast, D., and Saykally, R. J. Investigation of protein conformation and interactions with salts via X-ray absorption spectroscopy, *Proc. Natl. Acad. Sci. USA* **2010**, *107*, 14008-14013.

41. Gibb, C. L. D. and Gibb, B. C. Anion Binding to Hydrophobic Concavity is Central to the Salting-In Effects on Hofmeister Chaotropes *J. Am. Chem. Soc.* **2011**, *133*, 7344-7347.

42. Zhang, Y. Furyk, S. Sagle, L. B. Cho, Y. Bergbreiter, D. E. Cremer, P. S. Effects of Hofmeister anions on the LCST of PNIPAM as a function of molecular weight. *J. Phys. Chem. C* **2007** 111, 8916-8924.

Figure captions:

Figure 1: Simulated density maps of SO_4^{2-}, Cl^-, Br-, I^-, and SCN^- around terminated (left column) and non-terminated (right column) triglycine at an isovalue corresponding to three times the aqueous bulk ion density.

Figure 2: Simulated radial distribution functions to the three methylene groups with α-protons 1, 2, and 3 (top row) and preferential bindings to the corresponding adjacent regions (inset) of the terminated triglycine(bottom row) of SO_4^{2-}, Cl^-, Br-, I^-, and SCN^- ions.

Figure 3: Simulated radial distribution functions to the three methylene groups with α-protons 1, 2, and 3 (top row) and preferential binding to the corresponding adjacent regions (inset) of the non-terminated triglycine (bottom row) of SO_4^{2-}, Cl^-, Br-, I^-, and SCN^- ions.

Figure 4: Relative chemical shift changes of *N*-Ac-GGG-NH_2's alpha protons as function of salt concentration for 5 sodium salts.

Figure 5: Relative chemical shift changes of GGG's alpha protons as function of salt concentration for 5 sodium salts.

Figure 6: A schematic picture of binding sites of weakly hydrated anions (thiocyanate) and strongly hydrated anions (sulfate) at the capped vs. uncapped triglycine.

N-Ac-GGG-NH_2					GGG		
Na^+ counter-anion	K_d (mM)				K_d (mM)		
	α-proton 1	α-proton 2	α-proton 3		α-proton 1	α-proton 2	α-proton 3
SO_4^{2-}	-	-	-		70 ± 30	-	-
Cl^-	-	-	-		290 ± 240	-	-
Br^-	-	-	-		820 ± 560	-	-
I^-	> 1000	-	-		> 1000	-	-
SCN^-	> 1000	> 1000	-		> 1000	> 1000	-

Table 1. Fitted values for apparent dissociation constants, K_d, for alpha protons in different aqueous salt solutions with glycylglycylglycine and *N*-acetyl-glycylglycylglycinamide. A 95% confidence level was used to extract error bars from the fits. K_d.values above 1000 mM represent weaker binding and blanks were left when no binding could be observed at all within experimental error.

Figure 1:

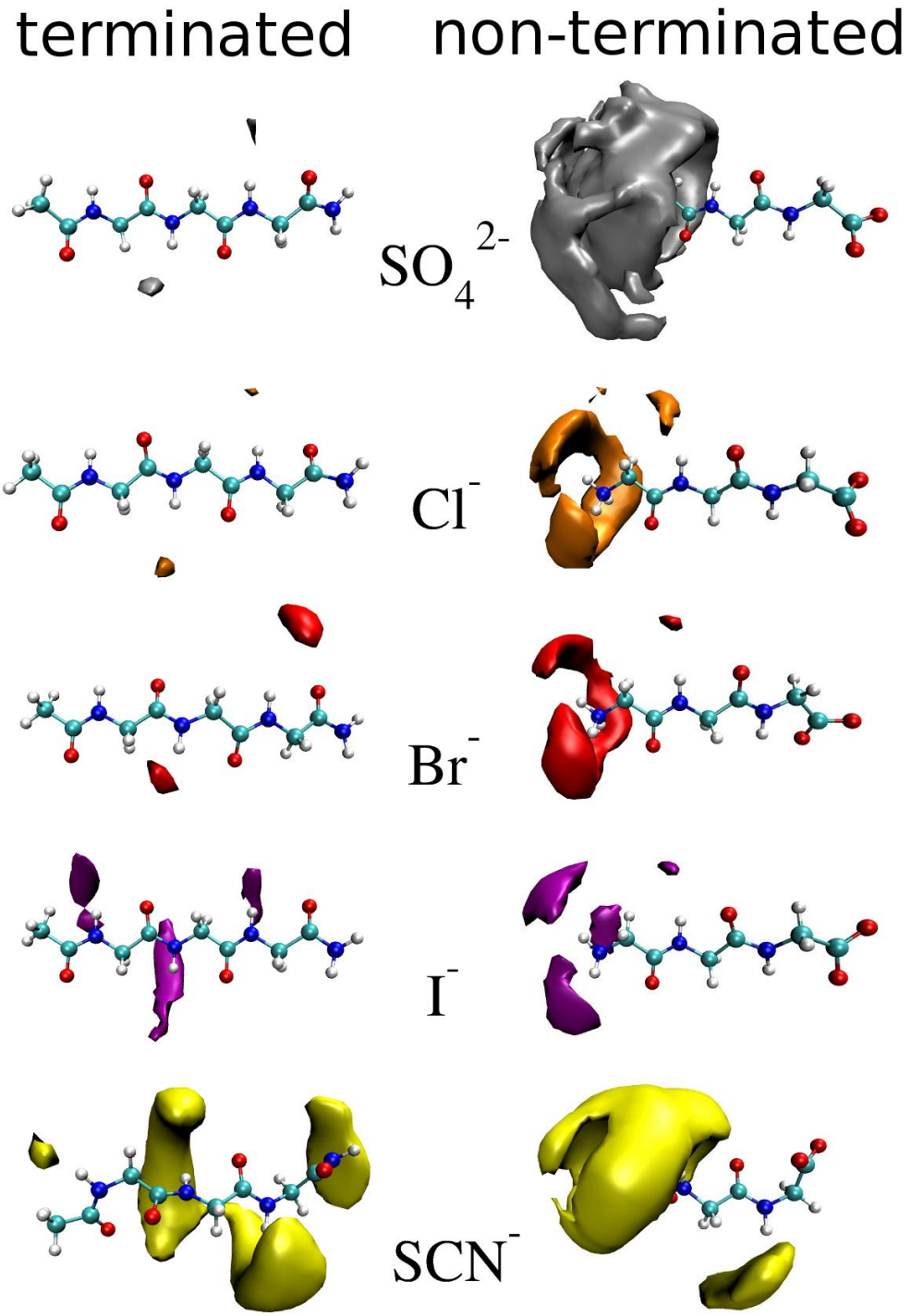

Figure 2:

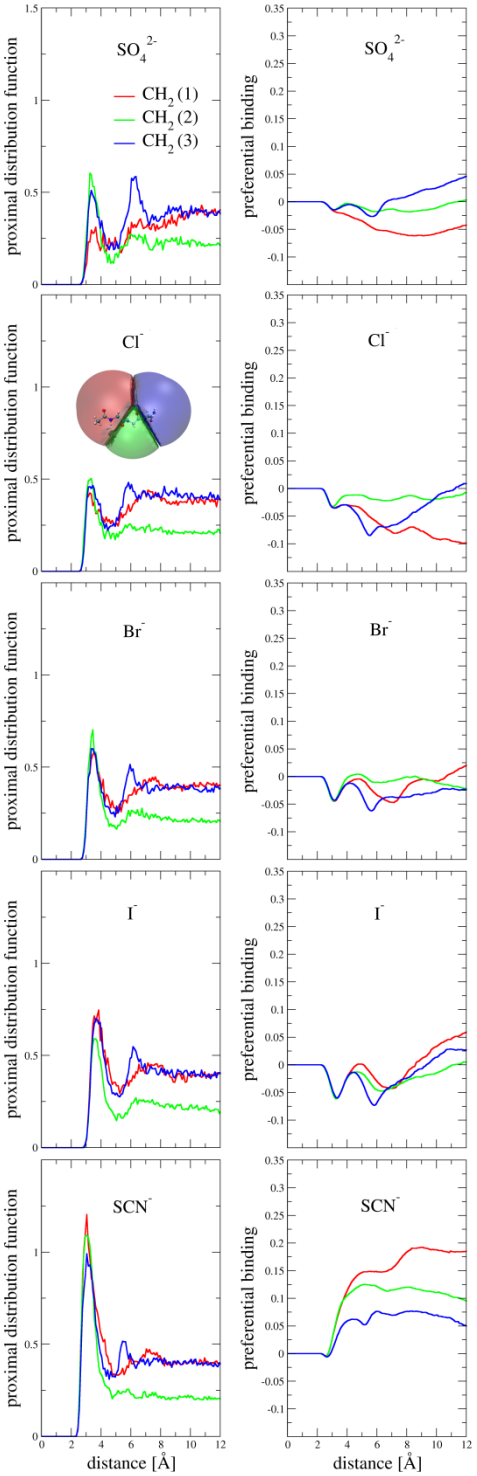
SO4 2-
CH2 (1)
CH2 (2)
CH2 (3)
Cl-
Br-
I-
SCN-
proximal distribution function
preferential binding
distance [Å]

Figure 3:

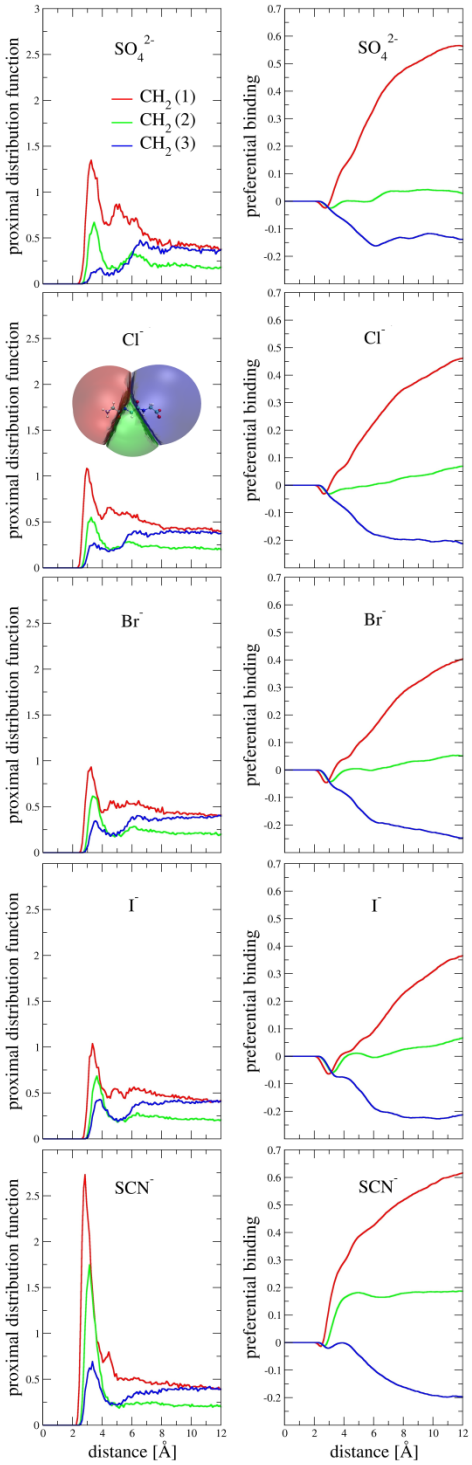
SO4 2-
CH2 (1)
CH2 (2)
CH2 (3)
Cl-
Br-
I-
SCN-
proximal distribution function
preferential binding
distance [Å]

Figure 4:

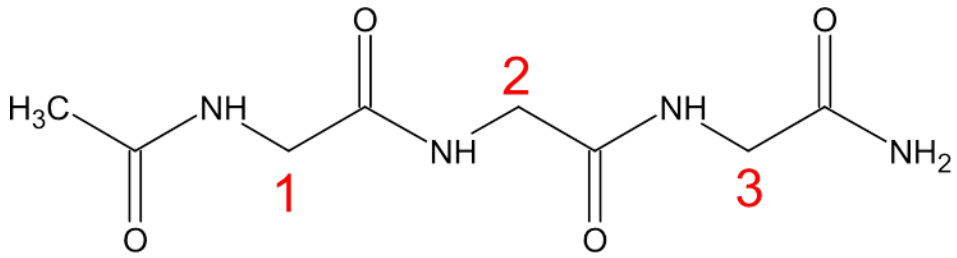

α-proton 1

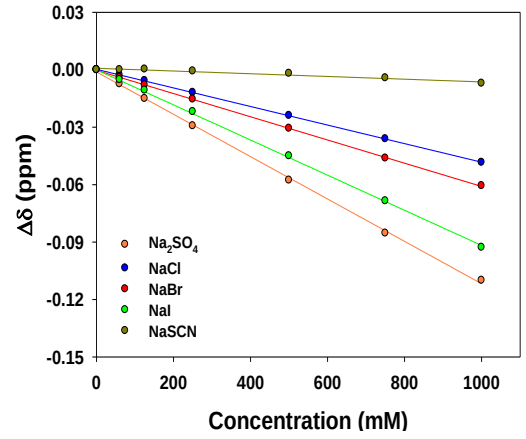

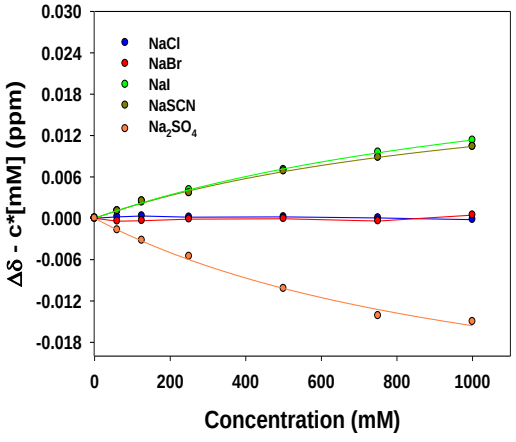

α-proton 2

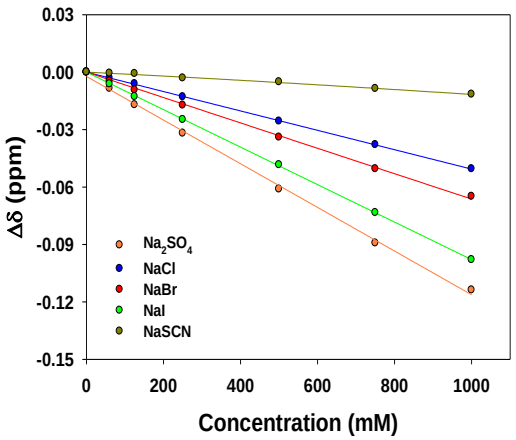

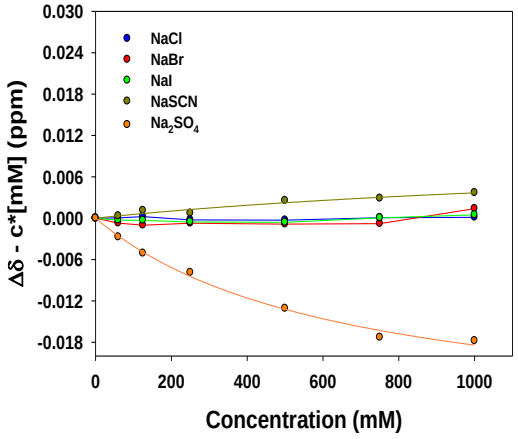

α-proton 3

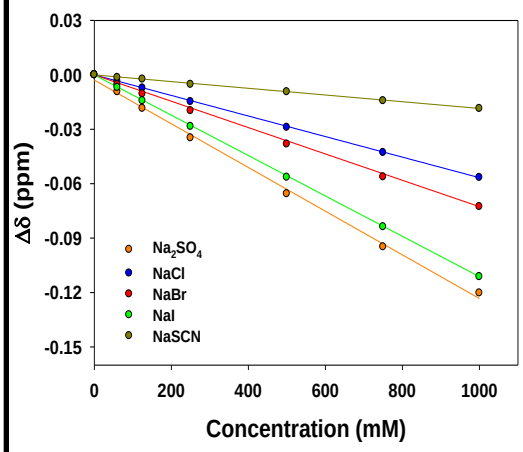

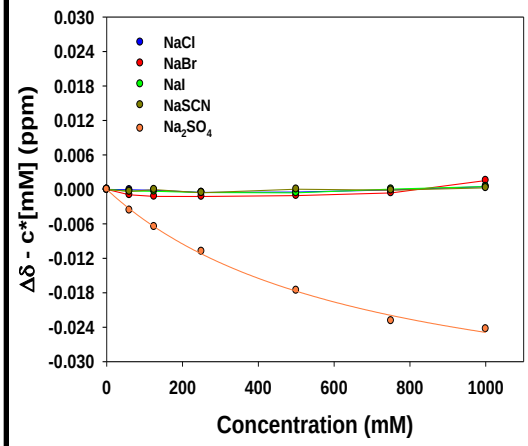

Figure 5:

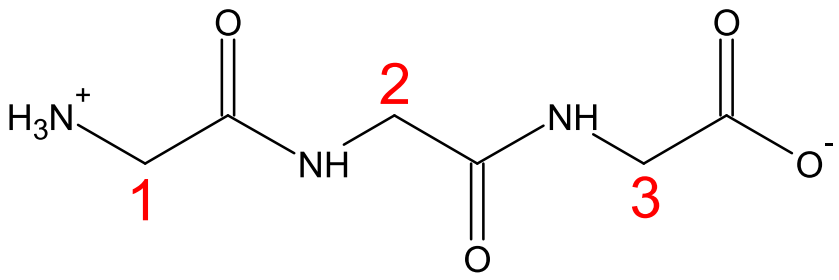
O
H_3N^+
2
NH
NH
O
O
O^-
1
3

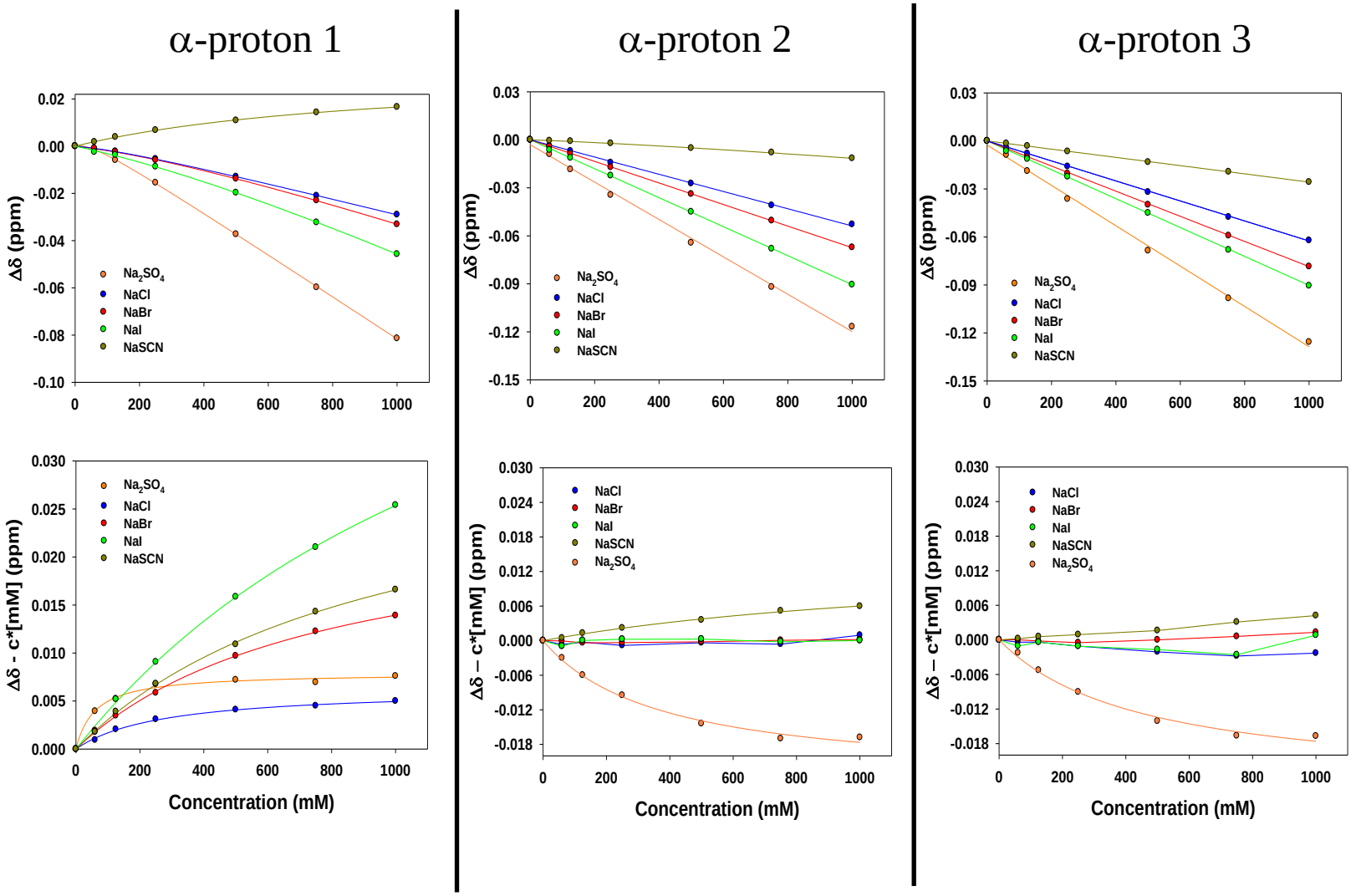
α-proton 1
α-proton 2
α-proton 3
Δδ (ppm)
Δδ - c*[mM] (ppm)
Δδ – c*[mM] (ppm)
Na_2SO_4
NaCl
NaBr
NaI
NaSCN
Concentration (mM)

Figure 6:

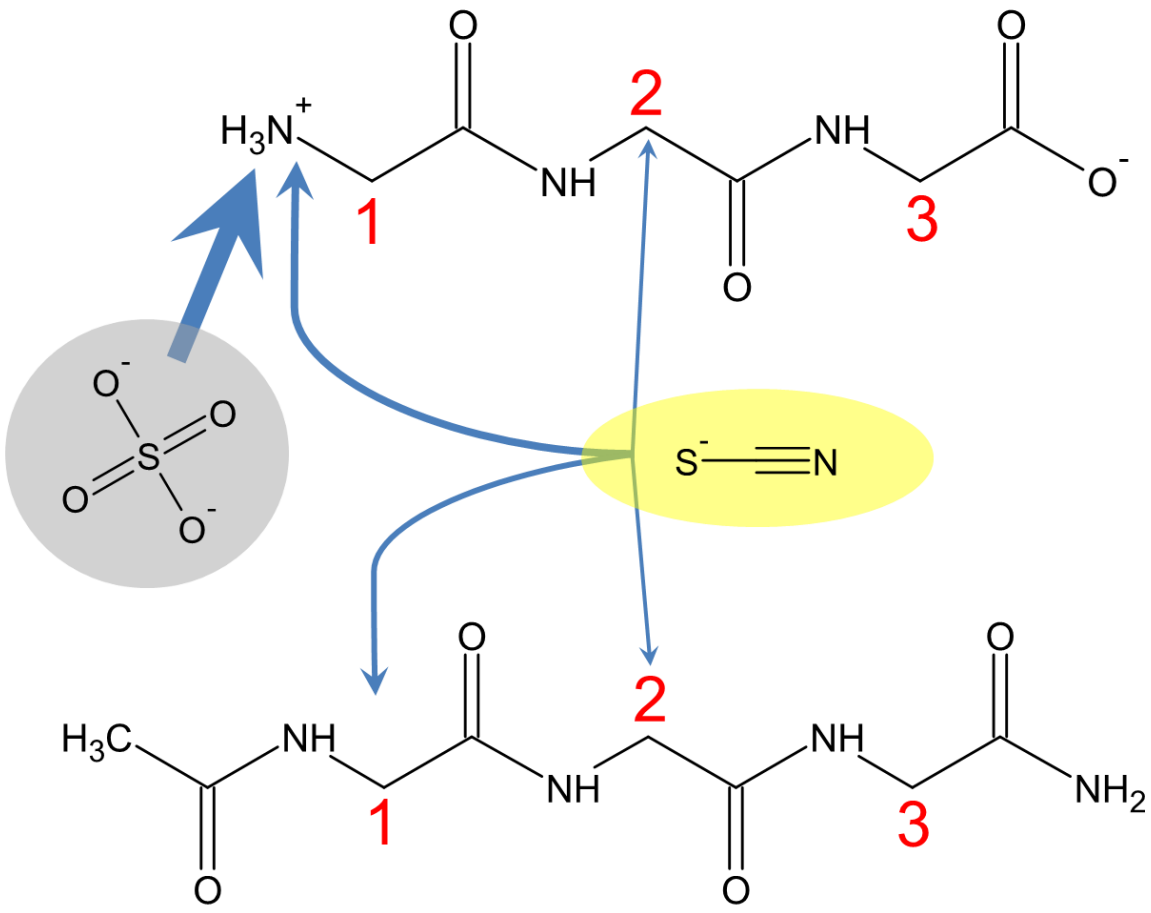

TOC graphics: